



Published in final edited form as:

*Biomaterials*. 2010 February ; 31(4): 602–607. doi:10.1016/j.biomaterials.2009.09.084.

## Altered Calcium Dynamics in Cardiac Cells Grown on Silane-Modified Surfaces

Melissa S. Ravenscroft-Chang<sup>1,2</sup>, Jayna Stohman<sup>2</sup>, Peter Molnar<sup>3</sup>, Anupama Natarajan<sup>3</sup>, Heather E. Canavan<sup>1</sup>, Maggie Teliska<sup>1</sup>, Maria Stancescu<sup>3</sup>, Victor Krauthamer<sup>2</sup>, and J.J. Hickman<sup>1,3</sup>

<sup>1</sup>The George Washington University, Department of Chemistry, Washington, DC 20052

<sup>2</sup>The Office of Science and Engineering Laboratories, Center for Devices and Radiological Health, Food and Drug Administration, Silver Spring, MD 20993

<sup>3</sup>University of Central Florida, NanoScience and Technology Center, Orlando, FL 32826

### Abstract

Chemically defined surfaces were created using self-assembled monolayers (SAMs) of hydrophobic and hydrophilic silanes as models for implant coatings, and the morphology and physiology of cardiac myocytes plated on these surfaces were studied *in vitro*. We focused on changes in intracellular Ca<sup>2+</sup> because of its essential role in regulating heart cell function. The SAM-modified coverslips were analyzed using X-ray Photoelectron Spectroscopy to verify composition. The morphology and physiology of the cardiac cells were examined using fluorescence microscopy and intracellular Ca<sup>2+</sup> imaging. The imaging experiments used the fluorescent ratiometric dye fura-2, AM to establish both the resting Ca<sup>2+</sup> concentration and the dynamic responses to electrical stimulation. A significant difference in excitation-induced Ca<sup>2+</sup> changes on the different silanated surfaces was observed. However, no significant change was noted based on the morphological analysis. This result implies a difference in internal Ca<sup>2+</sup> dynamics, and thus cardiac function, occurs when the composition of the surface is different, and this effect is independent of cellular morphology. This finding has implications for histological examination of tissues surrounding implants, the choice of materials that could be beneficial as implant coatings and understanding of cell-surface interactions in cardiac systems.

### Keywords

biocompatibility; calcium; cardiomyocyte; cell culture; image analysis; surface modification

## 1. Introduction

Biocompatibility is a central problem in tissue engineering as well as for coating for implants and other devices designed for *in vivo* applications [1-3]. To address the issue of

© 2009 Elsevier Ltd. All rights reserved.

\*Correspondence should be addressed to: James J. Hickman NanoScience Technology Center University of Central Florida 12424 Research Parkway, Suite 400 Orlando, FL 32826 jhickman@mail.ucf.edu.

**Publisher's Disclaimer:** This is a PDF file of an unedited manuscript that has been accepted for publication. As a service to our customers we are providing this early version of the manuscript. The manuscript will undergo copyediting, typesetting, and review of the resulting proof before it is published in its final citable form. Please note that during the production process errors may be discovered which could affect the content, and all legal disclaimers that apply to the journal pertain.

**Disclaimer:** The mention of commercial products, their sources, or their use in connection with material reported herein is not to be construed as either an actual or implied endorsement of such products by the Department of Health and Human Services.

biocompatibility, one can either choose a bulk composition that minimizes adverse interactions with the surrounding tissue or modify the surface of the existing material. In general, surface chemistry modifications have the advantage of creating favorable coatings that are independent of the bulk composition [4-6]. The use of surface modification strategies to address the issue of the biocompatibility of cardiac implant materials and devices has been gaining wider acceptance [7-11]. Specific examples of surface modification to address cardiac device biocompatibility include a 1995 study in which Tweden *et al.* demonstrated that cardiovascular implant fabrics modified with a synthetic RGD peptide (PepTite) promoted material passivation via accelerated healing [7]. In 1997, Vasudev *et al.* modified the surface of bovine pericardium with polyethylene glycol (PEG) through a glutaraldehyde linker to provide new ways of controlling calcification, which is known to cause bioprosthetic heart valve failure [8,9]. In 1998, Tseng *et al.* showed that amide and amine plasma modified expanded polytetrafluoroethylene (ePTFE) grafts enhanced the aortic bovine endothelial cell lining when placed inside an artificial circulatory system with well-defined flow conditions [10]. Investigators have also started to examine the role that surface modifications could play in improving the biocompatibility of cardiac pacemakers [12-16]. Stelzle *et al.* (1997) performed a two-prong study in which they demonstrated surface modification principles by (1) modifying the surfaces of pacemaker electrodes with a PEG layer with the eventual goal of suppressing inflammatory responses, and (2) photolithographically patterning the modified electrodes to affect selective adhesion of electrosensitive cells for stimulation and recording [12]. Extending the idea of applying surface modifications to pacemaker leads, van Wachem *et al.* (1998) used surface modified leads to achieve controlled release of the antibiotic gentamicin to examine the tissue reactions to bacteria-challenged leads [13]. However, the majority of these studies addressed healing and acceptance of the material, not the effect on the physiology / electrical properties of the cardiac tissue.

Our goal in this study was to investigate not only the morphological but the physiological effects of chemically defined surfaces on cardiac myocytes *in vitro*. We concentrated on intracellular  $Ca^{2+}$  signaling, because its central role in normal heart function and in diseases such as arrhythmias [17, 18]. Moreover, the cardiac system provides the opportunity for a physiological investigation that relates *in vitro* cellular studies to cardiac organ function because cardiac function depends upon  $[Ca^{2+}]$  as a key regulator [19]. Thus, investigators can obtain information concerning cardiac function based on *in vitro* studies using optical recording techniques that utilize fluorescent indicator dyes to conduct  $Ca^{2+}$  imaging experiments at the cellular level.

One type of surface modification strategy that has gained prevalence is the use of self-assembled monolayers (SAMs) for creating biocompatible surfaces. Silane-modified glass surfaces have been used to influence cell adhesion [20, 21], protein adsorption [22, 23], prosthetic device biocompatibility [24, 25], cell and antibody patterning [26-32] surface-bound biomembrane constructions [33], and for dental applications [34, 35]. The utilization of SAMs for modifying surfaces has been demonstrated on many types of surfaces (*e.g.* silicon dioxide [36, 37], gold [38-40], biodegradable polymers [41, 42], and other polymers such as Teflon [43, 44]). To date, few studies are available reporting their use in cardiac biocompatibility studies.

A self-assembled monolayer is a modifying layer composed of organic molecules, one molecule thick that can spontaneously form strong interactions or covalent bonds with reactive groups on an exposed surface. A large variety of functional groups or combination of functional groups can be located on the terminus opposite the attachment point of a SAM [36], and the chemical composition can be manipulated to systematically vary the surface

free energy [37]. SAMs can also be combined with fixed media components to establish a model system to study cellular interactions *in vitro* [20].

For this study we selected a fluorinated (hydrophobic) and an amine-containing (hydrophilic) silane in an effort to examine the differences in biocompatibility for two surfaces with widely differing surface energies. Because of the flexibility of the method and the wide selection of the available SAMs this technique can be further extended for the systematic study of surface effects on cardiac physiology which could have a significant impact on the design and implementation of cardiac assist devices.

## 2. Methods

### 2.1. Surface modification

Commercially available 1H, 1H', 2H, 2H'-perfluorodecyldimethylchlorosilane (15F), (Lancaster Synthesis, Inc., Windham, NH), Tridecafluoro-1,1,2,2-tetrahydroctyl-1-trichlorosilane (13F) (Gelest, Morrisville, PA) and trimethoxysilylpropyldiethylenetriamine (DETA), (United Chemicals, Bristol, PA) were selected as materials for SAM modifications. Anhydrous (99.8%) toluene or chloroform (Aldrich Chemical Company, Inc., Milwaukee, WI) was used for preparing silane deposition solutions under inert conditions using in a glove box under a nitrogen atmosphere. HPLC-grade acetone, HPLC-grade methanol, ACS-certified sulfuric acid, and ACS-certified hydrochloric acid (Fisher Scientific, Fair Lawn, NJ) were used as received for cleaning Red Label (22 × 22 mm, No. 1) cover glasses (Thomas Scientific, Swedesboro, NJ).

The procedures for both the cover glass cleaning and the silane derivatizations are provided in summary form below, as the more extensive details have been recently published [45]. The cover glasses were cleaned in a series of steps. Ceramic Coors racks (Thermo Fisher Scientific Inc., Waltham, MA) containing the cover glasses were soaked in a solution of 50/50 methanol/hydrochloric acid; rinsed with deionized water; soaked in concentrated sulfuric acid; rinsed with deionized water; boiled in deionized water; rinsed with acetone; and oven dried.

The cleaned cover glasses were then immersed in either a 0.1% (v/v) DETA in toluene or a 0.5% (v/v) 15F in toluene or 0.1% (v/v) 13F in toluene or 0.1% (v/v) 13F in chloroform. After immersion in solution, the DETA cover glasses were heated to just below the boiling temperature; rinsed with toluene; reheated to just below boiling temperature; and then oven dried. The 13F and 15F cover glasses were heated to just below boiling temperature; rinsed with toluene; and then oven dried.

### 2.2. Surface characterization

The elemental compositions of the SAM modifications were obtained using a VG Scientific XPS Model ESCALAB 220i-XL used in the high-energy resolution mode. The samples were charge compensated with a low energy electron gun. The takeoff angle was 35° and the spectra were normalized to the Si 2p peak of the substrate. Three points were taken on each coverslips. Duplicate coverslips were run. The contact angles were measured using a Ramé-Hart contact angle goniometer employing a sessile drop of deionized water. Advancing angles were measured and reported here.

### 2.3. Cell culture

Fertile eggs (CBT Farms, Inc., Chestertown, MD) were delivered and incubated for use at embryonic day 10. The cell culture medium was Leibovitz (L-15) Medium (Sigma Chemical Company, St. Louis, MO) supplemented with 2 mM L-glutamine-200mM (100x) and 50

units/mL penicillin-streptomycin (Gibco BRL, Life Technologies, Grand Island, NY). Other reagents used during the dissection included the following: trypsin (0.25%, 1x), certified fetal bovine serum, and Dulbecco's phosphate-buffered saline (D-PBS, 1x) without calcium and magnesium chlorides (Gibco BRL, Life Technologies, Grand Island, NY). The ratiometric  $\text{Ca}^{2+}$ -specific dye, fura-2 acetoxymethylester (AM) (Molecular Probes, Inc., Eugene, OR) was used with UV light excitation for the fluorescence imaging experiments [46, 47].

Cardiac cells were isolated from day 10 chick embryo whole hearts by dissociation in a 0.05% trypsin solution, as previously published [46, 47]. After dissociation, the cells were centrifuged, resuspended in the cell culture medium, and then plated (0.25 mL of cell suspension per  $22 \times 22$  mm cover glass) onto the SAM-modified cover glasses. The cells were allowed to adhere for 15 minutes and then the culture dishes were flooded with an additional 2 mL of culture medium and incubated at  $37^\circ\text{C}$ . The medium was removed and then replaced with fresh culture medium twice per week.

#### 2.4. Morphological analysis

Morphological analysis was performed on cardiac cells cultured on DETA and on 13F and 15F surfaces. Cell length was measured directly from epifluorescent photomicrographs obtained from fura-2 loaded cells. Other cell parameters (*i.e.*, cell perimeter, cell area, major and minor axes) were determined from the digital photomicrographs using Scion Image software (Scion Corporation, Frederick, MD). The cellular images were analyzed from data with borders imposed by relative light intensity as compared to the background to give maximum cellular area.

#### 2.5. Calcium imaging

The cells were incubated with the fura-2, AM (reconstituted to a 16.8 mM stock solution in DMSO and then diluted to a  $42 \mu\text{M}$  solution in L-15) solution for 25 minutes at  $37^\circ\text{C}$  [46-48]. After incubation, the fura-containing medium was removed, the cells were rinsed once with L-15, and a fresh L-15 solution was added to the culture dishes.

The epifluorescence microscope (Zeiss Axioplan, Thornwood, NY) was equipped with a cooled CCD-200 camera (Photometrics, Tucson, AZ) and fura-2 fluorescence filters with  $350 \pm 5$  nm and  $380 \pm 5$  nm excitation wavelengths. To determine the resting  $\text{Ca}^{2+}$  concentrations in the cells, the cells, loaded with the fura-2 AM, were excited with UV light and photographed alternately using the 380 nm and the 350 nm fluorescence filters. This 350/380 nm ratio method allowed for the calculation of the fractional change in fluorescence emission relative to the baseline fluorescence ( $F/F$ ) [46]. A parallel pair of platinum-iridium electrodes (1 cm separation) were submerged into the cell dish for the purpose of electrical stimulation [46]. The cells were electrically paced at select time intervals and the resulting changes in intracellular  $\text{Ca}^{2+}$  concentration were monitored.

### 3. Results

Our report on the response of cardiac cells to the different silane-modified surfaces proceeds through several steps, from the XPS characterization of the modified surfaces to the comparison of the cell morphology data and finally to the comparison of the differences in cell functions as seen by examining both resting calcium levels and intracellular dynamics following electrical stimulation.

### 3.1. Surface modification

High resolution XPS for the DETA surface preparation yielded a N(1s) spectra of  $1800 \pm 300$  counts when normalized to the Si(2p) peak with a peak area of 5000 (Figure 1), which was comparable to our earlier results [30]. High resolution XPS for 15F yielded a F(1s) signal of  $14,000 \pm 500$  compared to our previously reported value of around 14,200 counts when normalized to the Si(2p) peak with a peak area of 5000 (Figure 1) [30]. The contact angle values for DETA, 13F and 15F in Toluene and 13F in Chloroform were  $48.1 \pm 0.74$ ,  $106.4 \pm 0.64$  and  $99.0 \pm 3.32$ , respectively. We did not find any major difference in the surface characteristics between 13F and 15F in toluene based on the XPS and contact angle data; thus, we pooled the data from results obtained in the functional and morphological experiments together.

### 3.2. Morphology

Figure 2 provides examples of the morphological comparison between the fluorescent images of cardiac cells cultured on DETA and on a fluorinated surface at two different time points. To obtain quantitative cell morphology data, we analyzed the fluorescent images to assess cell area, perimeter and major/minor axes (Table 1). For the major/minor axes measurements, the software program (Scion Image) determined the lengths of the axes of the best-fitting ellipse for a given cell. We did not find differences in any of the measured morphological parameters between cardiac cells growing on the two defined surfaces on day 6 or day 9 *in vitro* (Table 1). However, while no significant changes in the cell area, perimeter or axes values were observed, an increased variance (square of the standard deviation) in cell length on DETA as compared to 13/15F was observed at both time points; an analysis of the distribution indicated that this was due to a statistically insignificant number of cells, and not germane to our study.

### 3.3. Cell function / Calcium imaging

In the fura-2 optical imaging experiments the cells were loaded with the fluorescent indicator dye, Fura-2 [48], which is UV-light excitable and exhibits an absorption shift upon binding to  $\text{Ca}^{2+}$  which can be observed at 350nm and 380nm. This ratiometric  $[\text{Ca}^{2+}]$  indicator can be used to establish the resting intracellular  $[\text{Ca}^{2+}]$ . Moreover, if the cells are electrically stimulated at select time intervals, the resulting changes in intracellular  $[\text{Ca}^{2+}]$  can be monitored.

The resting calcium imaging experiments established the baseline for the pacing experiments by establishing the level of  $\text{Ca}^{2+}$  that was present in the cells prior to electrical stimulation. The resting  $\text{Ca}^{2+}$  level of individual cardiac cells was calculated from the ratio of the 350nm-to-380nm UV data (Table 2). The calibration formula for resting  $\text{Ca}^{2+}$  concentration in nanomoles, as derived from the buffered calcium solutions, is  $[\text{Ca}^{2+}] = R(697) - 91$ , where R is the 350/380 ratio. Little difference was noted between the resting  $\text{Ca}^{2+}$  levels on the different surfaces at the measured time points. This indicated that the amount of cytosolic  $\text{Ca}^{2+}$  is the same for the cells on both surfaces.

The cardiac cells were stimulated by electrically pacing with a 1Hz, 6V signal with a duration of 5msec per pulse through the pair of submerged electrodes. The excitation-induced calcium transients were monitored by measuring changes in fluorescence intensity. Figure 3C graphically depicts the stimulation of day 6 cells. We observed a marked and consistent difference in intracellular  $\text{Ca}^{2+}$  dynamics on the two silanated surfaces. Both the amplitude and the width (measured at 50% amplitude) of the calcium transients evoked by electrical stimulation of cardiac myocytes were significantly different on DETA and on the fluorinated surface (Figure 3A and B).

## 4. Discussion

In this study we have developed an *in vitro* test system to evaluate the effect of surface coatings of possible cardiac implants on cardiac myocyte morphology and physiology. Surface characterization of the silanized surfaces confirmed our earlier findings concerning the high stability and consistent surface compositions and physical characteristics of the DETA and the 13F/15F modified surfaces. However, in contrast to our previous results with hippocampal neurons [30], embryonic chicken cardiac myocytes cultured on DETA or on fluorinated surfaces showed no morphological differences depending on the surface characteristics. Although this observation was unexpected, it is consistent with previous *in vivo* data concerning successful cardiac tissue integration with teflon valves, which had lower surface free energy, and successful cardiac integration with materials of higher surface free energy such as polyurethane. However, generally used histological examinations do not give insight to function of the cells in contact with these biomaterials in cardiac tissue integration studies.

In contrast to the common *in vivo* methods, our *in vitro* test system made not only morphological but also physiological studies possible. We chose intracellular calcium as the measured physiological parameter because it is central to all cardiac functions. Similarly to the morphological data we did not find any difference in the resting  $\text{Ca}^{2+}$  concentration between cardiac myocytes cultured on DETA or on the fluorinated surfaces. However, despite the similarities in cell morphology, combined electrophysiological/calcium imaging studies observed a significant difference in excitation-induced  $\text{Ca}^{2+}$  changes between the two surfaces. This result implies that a change in only surface composition can significantly affect the function or expression of  $\text{Ca}^{2+}$  channels in cardiac cells and/or alter the coupling between calcium influx and calcium release from the sarcoplasmic reticulum.

## Conclusions

This result has significant consequences for both histological analysis and biocompatibility. If the growth surface alone can cause an impairment of function without morphological consequences, then materials used in tissue engineering applications to repair cardiac tissue or for implanted assist devices may not cause a noticeable morphological difference *in vivo* but could alter function without measurable differences in classical histological analysis. Conversely, in histological examinations of tissue from impaired organs, the failure mode could be overlooked due to seemingly healthy tissue. Thus, extensive *in vitro* studies are necessary to investigate physiological effects of commonly used cardiac biomaterials. Moreover, surface modification strategies have to be developed which have the potential to improve the biocompatibility of the biomaterials already in use or under development.

## Acknowledgments

We gratefully acknowledge the support of the Department of Energy grant DEFG02-96ER14588 and NIH grant 5R01EB005459 for funding this work.

## REFERENCES

1. Shard AG, Tomlins PE. Biocompatibility and the efficacy of medical implants. *Regen Med.* 2006; 1(6):789–800. [PubMed: 17465760]
2. Kurella A, Dahotre NB. Review paper: Surface modification for bioimplants: The role of laser surface engineering. *J Biomater Appl.* 2005; 20(1):5–50. [PubMed: 15972362]
3. Shi GX, Cai Q, Wang CY, Lu N, Wang SG, Bei JZ. Fabrication and biocompatibility of cell scaffolds of poly(L-lactic acid) and poly(L-lactic-coglycolic acid). *Polym Adv Technol.* 2002; 13(3-4):227–32.

4. Ratner BD, Bryant SJ. Biomaterials: Where we have been and where we are going. *Annu Rev Biomed Eng.* 2004; 6:41–75. [PubMed: 15255762]
5. Harsch A, Calderon J, Timmons RB, Gross GW. Pulsed plasma deposition of allylamine on polysiloxane: a stable surface for neuronal cell adhesion. *J Neurosci Methods.* 2000; 98(2):135–44. [PubMed: 10880827]
6. Wilson CJ, Clegg RE, Leavesley DI, Percy MJ. Mediation of biomaterial-cell interactions by adsorbed proteins: A review. *Tissue Eng.* 2005; 11(1-2):1–18. [PubMed: 15738657]
7. Tweden KS, Harasaki H, Jones M, Blevitt JM, Craig WS, Pierschbacher M, et al. Accelerated healing of cardiovascular textiles promoted by an RGD peptide. *J Heart Valve Dis.* 1995; 4:s90–7. [PubMed: 8581220]
8. Vasudev SC, Chandy T, Sharma CP. Influence of polyethylene glycol graftings on the in vitro degradation and calcification of bovine pericardium. *J Biomater Appl.* 1997; 11(4):430–52. [PubMed: 9178094]
9. Vasudev SC, Chandy T. Effect of alternative crosslinking techniques on the enzymatic degradation of bovine pericardium and their calcification. *J Biomed Mater Res.* 1997; 35(3):357–69. [PubMed: 9138070]
10. Tseng DY, Edelman ER. Effects of amide and amine plasma-treated ePTFE vascular grafts on endothelial cell lining in an artificial circulatory system. *J Biomed Mater Res.* 1998; 42(2):188–98. [PubMed: 9773815]
11. Hsu LC. Biocompatibility in cardiopulmonary bypass. *J Cardiothorac Vasc Anesth.* 1997; 11(3): 376–82. [PubMed: 9161907]
12. Stelzle M, Wagner R, Nisch W, Jagermann W, Frohlich R, Schaldach M. On the chemical modification of pacemaker electrodes and patterned surface functionalization of planar substrates. *Biosens Bioelectron.* 1997; 12(8):853–65. [PubMed: 9421891]
13. van Wachem PB, Blaauw EH, de Vries-Hospers HG, Geerdes BP, Woloszko J, Verhoeven M, et al. Tissue reactions to bacteria-challenged implantable leads with enhanced infection resistance. *J Biomed Mater Res.* 1998; 41(1):142–53. [PubMed: 9641634]
14. Wagner R, Wu YL, Richter L, Pfohl T, Siegel S, Weissmuller J, et al. Wetting behaviour of carbohydrate-containing Si surfactants on perfluorinated surfaces and modification of rough metal surfaces by hydrophilised crosslinked polysiloxanes. *Chemie Ingenieur Technik.* 1998; 70(4):419–21.
15. Chou HA, Zavitz DH, Ovadia M. In vivo CH<sub>3</sub>(CH<sub>2</sub>)<sub>11</sub>SAu SAM electrodes in the beating heart: In situ analytical studies relevant to pacemakers and interstitial biosensors. *Biosens Bioelectron.* 2003; 18(1):11–21. [PubMed: 12445440]
16. Schoenfisch MH, Ovadia M, Pemberton JE. Covalent surface chemical modification of electrodes for cardiac pacing applications. *J Biomed Mater Res.* 2000; 51(2):209–15. [PubMed: 10825220]
17. Scoote M, Williams AJ. Myocardial calcium signalling and arrhythmia pathogenesis. *Biochem Biophys Res Commun.* 2004; 322(4):1286–309. [PubMed: 15336976]
18. Clusin WT. Calcium and cardiac arrhythmias: DADs, EADs, and alternans. *Crit Rev Clin Lab Sci.* 2003; 40(3):337–75. [PubMed: 12892319]
19. Sparks, HV.; Rooke, TW. *Essentials of Cardiovascular Physiology.* University of Minnesota Press; Minneapolis, MN: 1987.
20. Schaffner AE, Barker JL, Stenger DA, Hickman JJ. Investigation of the factors necessary for growth of hippocampal neurons in a defined system. *J Neurosci Methods.* 1995; 62(1-2):111–9. [PubMed: 8750092]
21. Jenney CR, DeFife KM, Colton E, Anderson JM. Human monocyte/macrophage adhesion, macrophage motility, and IL-4-induced foreign body giant cell formation on silane-modified surfaces in vitro. *J Biomed Mater Res.* 1998; 41(2):171–84. [PubMed: 9638521]
22. Collier TO, Jenney CR, DeFife KM, Anderson JM. Protein adsorption on chemically modified surfaces. *Biomed Sci Instrum.* 1997; 33:178–83. [PubMed: 9731356]
23. Culp LA, Sukenik CN. Cell type-specific modulation of fibronectin adhesion functions on chemically-derivatized self-assembled monolayers. *J Biomater Sci Polym Ed.* 1998; 9(11):1161–76. [PubMed: 9860178]

24. Atkinson JR, Cicek RZ. Silane Crosslinked Polyethylene for Prosthetic Applications .2. Creep and Wear Behavior and a Preliminary Molding Test. *Biomaterials*. 1984; 5(6):326–35. [PubMed: 6525392]
25. Okamoto T, Tashiro M, Sakanashi Y, Tanimoto H, Imaizumi T, Sugita M, et al. A new heparin-bonded dense membrane lung combined with minimal systemic heparinization prolonged extracorporeal lung assist in goats. *Artif Organs*. 1998; 22(10):864–72. [PubMed: 9790085]
26. Chung DJ, Matsuda T. Microfabricated surface designs for controlled cell culture. *Polym-Korea*. 1999; 23(1):137–44.
27. Corey JM, Wheeler BC, Brewer GJ. Micrometer resolution silane-based patterning of hippocampal neurons: Critical variables in photoresist and laser ablation processes for substrate fabrication. *IEEE Trans Biomed Eng*. 1996; 43(9):944–55. [PubMed: 9214810]
28. Chen CS, Mrksich M, Huang S, Whitesides GM, Ingber DE. Geometric control of cell life and death. *Science*. 1997; 276(5317):1425–8. [PubMed: 9162012]
29. Thomas CH, McFarland CD, Jenkins ML, Rezania A, Stelle JG, Healy KE. The role of vitronectin in the attachment and spatial distribution of bone-derived cells on materials with patterned surface chemistry. *J Biomed Mater Res*. 1997; 37:81–93. [PubMed: 9335352]
30. Ravenscroft MS, Bateman KE, Shaffer KM, Schessler HM, Jung DR, Schneider TW, et al. Developmental neurobiology implications from fabrication and analysis of hippocampal neuronal networks on patterned silane- modified surfaces. *J Am Chem Soc*. 1998; 120(47):12169–77.
31. Mooney JF, Hunt AJ, McIntosh JR, Liberko CA, Walba DM, Rogers CT. Patterning of functional antibodies and other proteins by photolithography of silane monolayers. *Proc Natl Acad Sci U S A*. 1996; 93(22):12287–91. [PubMed: 8901573]
32. Kleinfeld D, Kahler KH, Hockberger PE. Controlled outgrowth of dissociated neurons on patterned substrates. *J Neurosci*. 1988; 8(11):4098–120. [PubMed: 3054009]
33. Kuhl TL, Majewski J, Wong JY, Steinberg S, Leckband DE, Israelachvili JN, et al. A neutron reflectivity study of polymer-modified phospholipid monolayers at the solid-solution interface: Polyethylene glycol-lipids on silane-modified substrates. *Biophys J*. 1998; 75(5):2352–62. [PubMed: 9788930]
34. Eikenberg S, Shurtleff J. Effect of hydration on bond strength of a silane-bonded composite to porcelain after seven months. *Gen Dent*. 1996; 44(1):58–61. [PubMed: 8940571]
35. Petersson LG, Twetman S, Pakhomov GN. The efficiency of semiannual silane fluoride varnish applications: a two-year clinical study in preschool children. *J Public Health Dent*. 1998; 58(1): 57–60. [PubMed: 9608447]
36. Ulman, A. *Introduction to Ultrathin organic Films*. Academic Press, Inc.; San Diego: 1991.
37. Stenger DA, Georger JH, Dulcey CS, Hickman JJ, Rudolph AS, Nielsen TB, et al. Coplanar Molecular Assemblies of Aminoalkylsilane and Perfluorinated Alkylsilane - Characterization and Geometric Definition of Mammalian-Cell Adhesion and Growth. *J Am Chem Soc*. 1992; 114(22): 8435–42.
38. Bain CD, Whitesides GM. Correlations between Wettability and Structure in Monolayers of Alkanethiols Adsorbed on Gold. *J Am Chem Soc*. 1988; 110(11):3665–6.
39. Poirier GE, Pylant ED. The self-assembly mechanism of alkanethiols on Au(111). *Science*. 1996; 272(5265):1145–8. [PubMed: 8662446]
40. Mrksich M. Using self-assembled monolayers to understand the biomaterials interface. *Curr Opin Colloid Interface Sci*. 1997; 2(1):83–8.
41. Piskin E. Biodegradable Polymers as Biomaterials. *J Biomater Sci Polym Ed*. 1995; 6(9):775–95. [PubMed: 7772566]
42. Ikada Y. Surface Modification of Polymers for Medical Applications. *Biomaterials*. 1994; 15(10): 725–36. [PubMed: 7986935]
43. Vargo TG, Thompson PM, Gerenser LJ, Valentini RF, Aebischer P, Hook DJ, et al. Monolayer Chemical Lithography and Characterization of Fluoropolymer Films. *Langmuir*. 1992; 8(1):130–4.
44. Vargo TG, Bekos EJ, Kim YS, Ranieri JP, Bellamkonda R, Aebischer P, et al. Synthesis and Characterization of Fluoropolymeric Substrata with Immobilized Minimal Peptide Sequences for Cell-Adhesion Studies .1. *J Biomed Mater Res*. 1995; 29(6):767–78. [PubMed: 7593014]



45. Das M, Molnar P, Devaraj H, Poeta M, Hickman JJ. Electrophysiological and Morphological Characterization of Rat Embryonic Motoneurons in a Defined System. *Biotechnol Prog.* 2003; 19:1756–61. [PubMed: 14656152]
46. Krauthamer V, Jones JL. Effects of biphasic electric shocks on calcium changes in cultured cardiac myocytes. *In Vitro Mol Toxicol.* 1998; 11(3):221–8.
47. Krauthamer V, Jones JL. Calcium dynamics in cultured heart cells exposed to defibrillator-type electric shocks. *Life Sci.* 1997; 60(22):1977–85. [PubMed: 9180351]
48. Grynkiewicz G, Poenie M, Tsien RY. A new generation of Ca<sup>2+</sup> indicators with greatly improved fluorescence properties. *J Biol Chem.* 1985; 260(6):3440–50. [PubMed: 3838314]

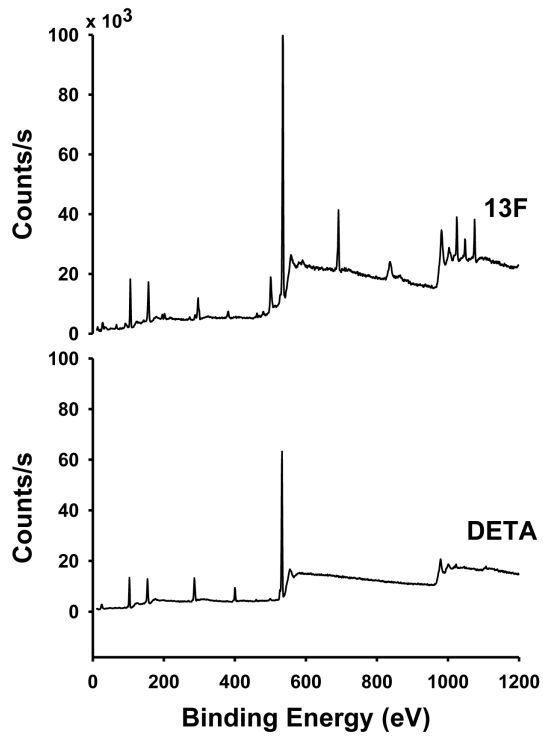


**Figure 1.**  
Representative XPS survey spectra of DETA and 13F-modified glass coverslips

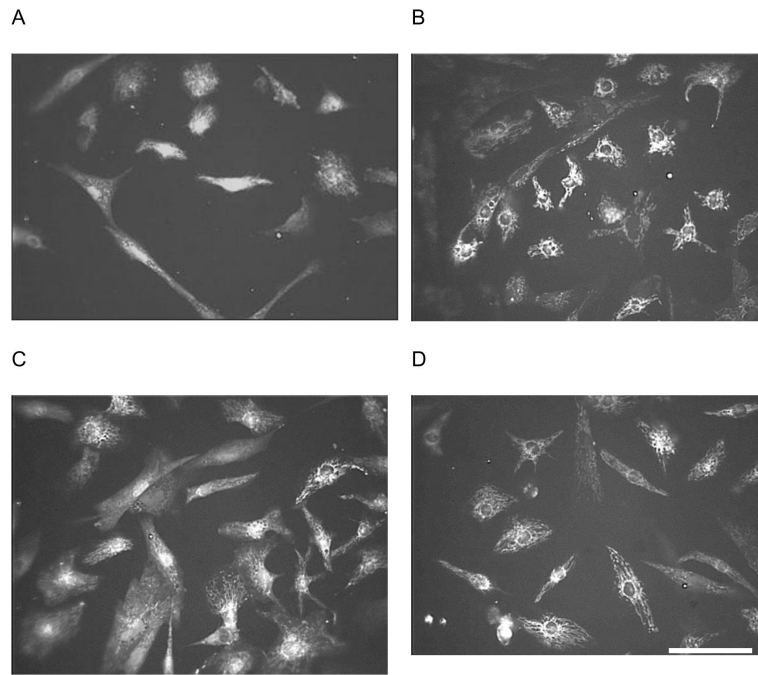


**Figure 2.** Representative epifluorescent images of fura-2, AM-stained chick cardiac cells. A: DETA, day 6 *in vitro*, B: 15F, day 6 *in vitro*, C: DETA, day 9 *in vitro*, D: 15F, day 9 *in vitro*. Scale bar: 50  $\mu\text{m}$ .

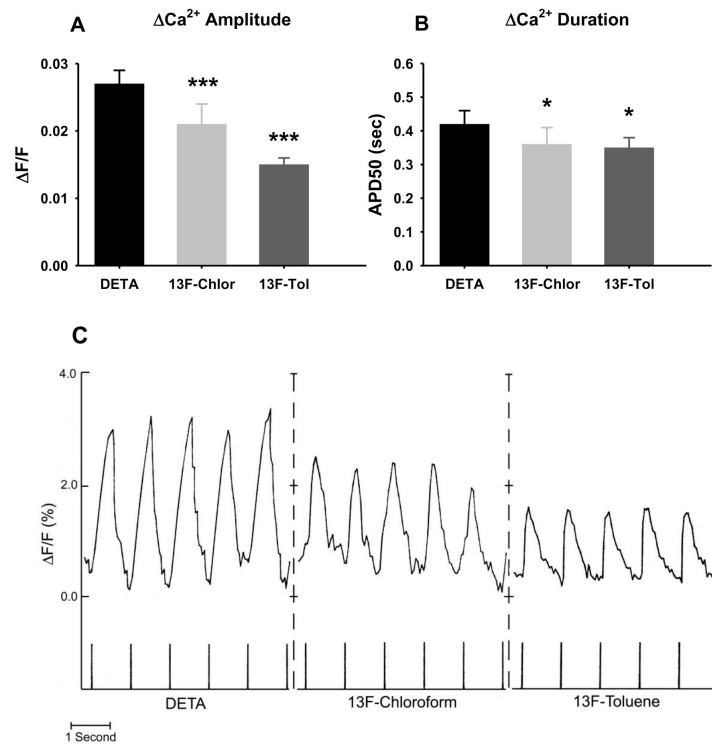


**Figure 3.**

Normalized change in fluorescence with electrical pacing for day 6 cardiac cells on DETA and on 13F-modified surfaces. C: Representative recording traces. Chicken embryonic cardiac myocytes cultured on silane-modified surfaces were incubated with fura-2, AM and electrically stimulated at 1Hz with a 6V, 5msec pulse using extracellular stimulating electrodes. Change in intracellular  $\text{Ca}^{2+}$  concentration was measured as  $\text{F}/\text{F}$  ratio. A: Differences in the amplitude of the calcium transients evoked by the electrical stimulation. B: Differences in the width (measured at half amplitude, APD50) of the calcium transients. The DETA coverslips were compared to the 13F-modified coverslips using the Student's t-test: \*=  $P < 0.05$ , \*\*\*=  $P < 0.0001$ .

**Table 1**

Comparison of morphology data obtained for heart cells cultured on DETA and 13/15F at two time points. The data is presented as average values (n is provided in each case) with their standard deviations.

CELL PARAMETERS	DAY 6		DAY 9	
	DETA	13/15F	DETA	13/15F
Number of Cells (n)	41	51	53	66
Area ( $\mu\text{m}^2$ )	1134.5 $\pm$ 717.3	1190.1 $\pm$ 612.2	1406.2 $\pm$ 501.7	1492.5 $\pm$ 522.6
Perimeter ( $\mu\text{m}$ )	191.1 $\pm$ 84.2	206.6 $\pm$ 88.7	222.1 $\pm$ 70.4	240.6 $\pm$ 74.9
Ratio: Area/Perimeter	5.7 $\pm$ 1.7	5.8 $\pm$ 1.9	6.4 $\pm$ 1.2	6.3 $\pm$ 1.5
Major Axis ( $\mu\text{m}$ )	57.4 $\pm$ 27.8	55.0 $\pm$ 20.1	58.5 $\pm$ 15.4	66.3 $\pm$ 16.9
Minor Axis ( $\mu\text{m}$ )	24.3 $\pm$ 8.6	27.3 $\pm$ 8.4	30.6 $\pm$ 7.1	29.2 $\pm$ 8.5
Ratio:Major/Minor Axes	2.6 $\pm$ 1.6	2.2 $\pm$ 1.2	2.1 $\pm$ 0.91	2.5 $\pm$ 1.2

**Table 2**

Comparison of resting  $\text{Ca}^{2+}$  levels for cardiac cells on DETA and 13/15F at Day 6 and 9 in vitro.

CELL PARAMETERS	DAY 6		DAY 9	
	DETA	15F	DETA	15F
Resting $[\text{Ca}^{2+}]$ (nM)	129 ± 39	141 ± 59	148 ± 71	125 ± 62
Number of Cells (n)	32	32	42	42